Neuron, Vol. 38, 447–460, May 8, 2003, Copyright ©2003 by Cell Press

Hippocampal LTP Is Accompanied by Enhanced F-Actin Content within the Dendritic Spine that Is Essential for Late LTP Maintenance In Vivo

Yugo Fukazawa,[1,2,6] Yoshito Saitoh,[1,6] Fumiko Ozawa,[1] Yasuhiko Ohta,[3] Kensaku Mizuno,[4] and Kaoru Inokuchi[1,5,*]

[1]Mitsubishi Kagaku Institute of Life Sciences (MITILS)
Machida, Tokyo 194-8511
Japan
[2]Division of Cerebral Structure
National Institute for Physiological Sciences
Okazaki 444-8585
Japan
[3]Laboratory of Animal Science
Tottori University
Tottori 680-8553
Japan
[4]Department of Biomolecular Sciences
Graduate School of Life Sciences
Tohoku University
Sendai 980-8578
Japan
[5]Graduate School of Environment and Information Sciences
Yokohama National University
Yokohama 240-8501
Japan

Summary

The dendritic spine is an important site of neuronal plasticity and contains extremely high levels of cytoskeletal actin. However, the dynamics of the actin cytoskeleton during synaptic plasticity and its in vivo function remain unclear. Here we used an in vivo dentate gyrus LTP model to show that LTP induction is associated with actin cytoskeletal reorganization characterized by a long-lasting increase in F-actin content within dendritic spines. This increase in F-actin content is dependent on NMDA receptor activation and involves the inactivation of actin depolymerizing factor/cofilin. Inhibition of actin polymerization with latrunculin A impaired late phase of LTP without affecting the initial amplitude and early maintenance of LTP. These observations suggest that mechanisms regulating the spine actin cytoskeleton contribute to the persistence of LTP.

Introduction

Synaptic plasticity, a long-lasting change in synaptic efficacy in response to neural activity, is thought to be involved in a wide variety of brain functions including learning and memory. It appears that the dendritic spine, a specialized structure in the mature brain on which the majority of excitatory glutamatergic synapses is formed, is a critical site for synaptic plasticity (Halpain, 2000; Matus, 2000; van Rossum and Hanisch, 1999). A pronounced characteristic of the dendritic spine is an enrichment of cytoskeletal actin, and indeed the actin filament (F-actin) is the major cytoskeletal element in the dendritic spine (Fifkova and Morales, 1992; Matus et al., 1982). The F-actin is particularly prevalent in the spine head, the postsynaptic density (PSD), and the spine apparatus (Capani et al., 2001). It appears that the cytoskeleton formed by the F-actin in the dendritic spine is more dynamic than was previously thought. For example, the dendritic spines of cultured hippocampal neurons exhibit a rapid actin-based motility that is regulated by glutamate receptor activation (Fischer et al., 1998, 2000). The ability of the dendritic spine to swiftly alter its actin cytoskeleton is also shown by the remarkable fact that over 80% of the spine actin is in a dynamic state with a turnover time of less than a minute (Star et al., 2002). That the F-actin in the dendritic spine contributes to synaptic plasticity is suggested by studies showing that actin assembly plays an essential role in the molecular process underlying hippocampal long-term potentiation (LTP), a typical form of synaptic plasticity. In these studies, actin assembly was pharmacologically inhibited and it was found that this either decreases the LTP magnitude or impairs early LTP maintenance in hippocampal slice preparations (Kim and Lisman, 1999; Krucker et al., 2000).

How the cytoskeletal actin in the dendritic spine could contribute to synaptic plasticity is unclear, but there are several possibilities. First, it probably plays a central role in the morphological changes of the spine that occur in response to a variety of neural activity including the electrical stimuli that evoke LTP (Colicos et al., 2001; Engert and Bonhoeffer, 1999; Geinisman et al., 1996; Maletic-Savatic et al., 1999; Toni et al., 1999; Trachtenberg et al., 2002; Wu et al., 2001). These morphological changes, which may reflect the formation of new synapses, include the protrusion of new dendritic filopodia and spine outgrowth. They are input specific and correlate with the induction of LTP. These changes in spine morphology are mainly mediated by the actin cytoskeleton (Colicos et al., 2001). Another way the actin cytoskeleton could contribute to synaptic plasticity is by mediating the exocytosis and endocytosis of AMPA-type glutamate receptors (AMPARs) at postsynaptic sites. These events are important in the maintenance of early LTP (E-LTP) (Carroll et al., 2001; Malinow et al., 2000; Sheng et al., 2001), and endocytotic and exocytotic processes depend in general on the actin cytoskeleton (Cremona and De Camilli, 2001; Qualmann et al., 2000; Schafer, 2002). The actin filament could also serve as a path for local protein trafficking within the dendritic spine (Kaech et al., 2001; Langford and Molyneaux, 1998). Finally, as F-actin acts as an anchor for postsynaptic macromolecular complexes, a change in the actin cytoskeleton would probably alter the functional state of postsynaptic proteins, which in turn could affect synaptic efficacy (Allison et al., 1998; Halpain, 2000; Lisman and Zhabotinsky, 2001; van Rossum and Hanisch, 1999).

Hippocampal LTP consists of at least two distinct phases, namely, an early LTP (E-LTP) phase that is inde-

*Correspondence: kaoru@libra.ls.m-kagaku.co.jp
[6]These authors contributed equally to this work.

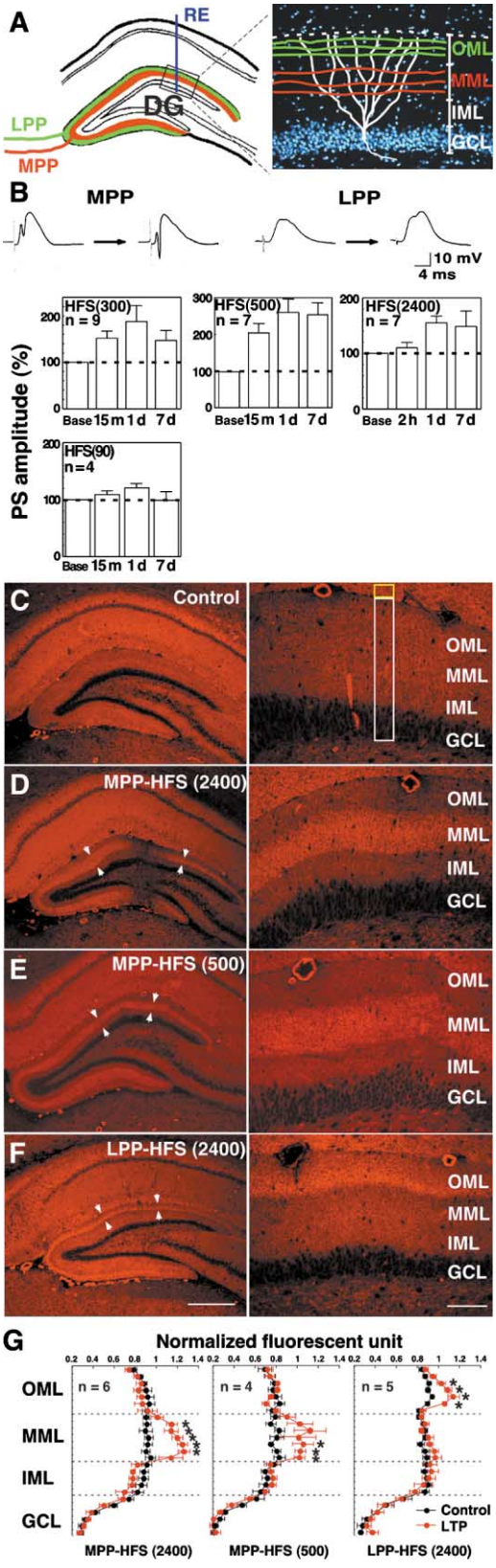

Figure 1. LTP Is Accompanied by an Increase in Histochemical Reactivity to F-Actin in an Input-Specific Manner

(A) Left: anatomical organization of the entorhinal-dentate gyrus pathway. Right: schematic illustration of a single granule cell in the upper blade of the dentate gyrus and the incoming presynaptic fibers MPP (red) and LPP (green) originating from the medial and lateral entorhinal cortex, respectively. This figure is superimposed onto a microscopic image stained with H33258 to show the nuclear distribution of individual cells. The broken line indicates the hippocampal fissure. Abbreviations: DG, dentate gyrus; RE, recording electrode; OML, outer molecular layer; MML, middle molecular layer; IML, inner molecular layer; and GCL, granule cell layer.

(B) Duration of MPP-LTP. Population spike (PS) amplitude was monitored at the times indicated after the delivery of HFS. The potentiation of PS amplitudes persisted for at least 1 week when a strong HFS [HFS (2400), HFS (500), or HFS (300)] was delivered. When a weak HFS [HFS (90)] was delivered, the potentiation of PS amplitudes persisted for 1 day but decayed to basal level within 1 week. Typical fEPSP traces evoked before (left) and 45 min after (right) HFS (2400) of the MPP or LPP are also shown (top panel).

(C–F) The HFS indicated was delivered to the MPP (D and E) or LPP (F) fibers to elicit LTP at the MML or OML synapses, respectively. The brain was dissected 45 min after beginning the HFS and subjected to phalloidin-TRITC staining. Left: CCD images showing phalloidin reactivity (F-actin) in the LTP side (D–F) and control (contralateral) side (C) of the hippocampus are shown. Arrowheads indicate areas that have an increased phalloidin reactivity. The bar in (F) represents 500 μm. Right: magnified images showing phalloidin reactivity 45 min after beginning the HFS. Bar in (F) represents 100 μm.

(G) The fluorescent intensity of phalloidin-TRITC was quantified across the molecular and granule cell layers. A schematic illustration of an area of fluorometric measurement (white rectangle) and a reference area (upper small square) whose mean fluorescent intensity was used for normalization are shown in (C) (right). The brain was dissected 45 min after beginning the HFS indicated. The fluorescence intensity of the phalloidin-TRITC signal (0–256 grading) at each pixel was divided by the averaged fluorescence intensity in the reference area and expressed as a normalized fluorescence unit. Data (mean ± SEM) from the LTP and the control (contralateral) sides of the dentate gyrus are shown in red or black, respectively. *, $p < 0.05$, compared with control side, t test. n, number of animals used for quantification.

pendent of macromolecule synthesis, and a late LTP (L-LTP) phase that is dependent on protein synthesis (Bailey et al., 1996). E-LTP lasts 2–3 hr in hippocampal slice preparations and several hours in intact animals, while L-LTP persists for several hours in slices and days or even weeks in unanesthetized animals (Abraham et al., 1993; Frey et al., 1993, 1996; Krug et al., 1984; Matsuo et al., 2000; Nguyen et al., 1994; Nguyen and Kandel, 1996). A number of genes that are upregulated following L-LTP induction have been identified (Matsuo et al., 2000; Nedivi et al., 1993; Qian et al., 1993; Yamagata et al., 1993). Interestingly, they include the genes encoding the actin-associated proteins synaptopodin and Arc (Link et al., 1995; Lyford et al., 1995; Yamazaki et al., 2001). This suggests that the spine actin cytoskeleton is not only involved in the rapid and reversible motility that occurs within seconds or minutes, but it may also be involved in morphological changes that occur slowly and are sustained over hours and days to maintain the L-LTP.

In this paper we induced LTP in the dentate gyrus of living animals and examined the effect of this on the actin cytoskeleton in the spine. We observed that F-actin content of spines was increased and found that this is mediated in part by the inactivation of actin depolymerizing factor (ADF)/cofilin, and inhibition of actin polymerization by latrunculin A treatment blocked the late phase

of LTP. These results indicate the crucial role that activity-dependent regulation of spine actin dynamics plays in synaptic plasticity.

Results

F-Actin Content in Synaptic Layers Undergoes a Net Increase after LTP Induction

To study actin cytoskeletal changes during neural activity-dependent synaptic plasticity, we examined LTP in the dentate gyrus of freely moving unanesthetized rats. In the dentate gyrus of the hippocampus, each granule cell receives two distinct inputs from the entorhinal cortex known as the medial and lateral perforant pathways (MPP and LPP, respectively) (Figure 1A; Hjorth, 1972; Hjorth and Jeune, 1972; McNaughton, 1980; McNaughton and Barnes, 1977; Steward, 1976). MPP fibers originate from the medial entorhinal area and terminate in the middle one-third of the molecular layer (MML) of the hippocampus while the LPP fibers originate from the lateral entorhinal area and terminate in the outer one-third of the molecular layer (OML). As noted previously by McNaughton (McNaughton and Barnes, 1977) and confirmed by our own recordings (Figure 1B, top panel), electrical stimulation of these fibers produces a characteristic waveform of evoked field excitatory postsynaptic potential (fEPSP) superimposed by a population spike. The fEPSP traces obtained by stimulating the MPP fibers show shorter latent periods prior to the peak and shorter half-widths compared with the traces following LPP stimulation. Furthermore, high-frequency stimulation (HFS) of the MPP and the LPP fibers specifically results in LTP at the MML (Figure 1B, bottom panel) and OML (not shown) synapses, respectively (also see McNaughton and Barnes, 1977). We used this model of LTP in unanesthetized animals throughout this work except when we examined the effect of drug infusion on LTP persistence, which required the use of urethane-anesthetized animals (Figures 5, 6D, and 6E).

We found that when a strong HFS [HFS (2400), HFS (500), or HFS (300); numbers in parenthesis indicate the total number of stimulation pulses, see Experimental Procedures for details] was delivered to MPP fibers, L-LTP was elicited in MML synapses that lasted more than a week (Figure 1B), which confirms previous observations (Abraham et al., 1993; Matsuo et al., 2000). Histochemical examination of the dentate gyrus of these rats revealed that the MML had marked increase in reactivity to phalloidin, a specific probe for F-actin [Figures 1C–1E, 45 min after the beginning of HFS; see also Figure 7A for HFS (300)]. In addition, the quantification of the average fluorescence intensities of the molecular and granule cell layers in the upper blade of the phalloidin-stained dentate gyrus revealed that the phalloidin reactivity of the MML had increased significantly (Figure 1G). Similarly, HFS (2400) of the LPP fiber, which elicits L-LTP in the OML synapses (data not shown), significantly enhanced phalloidin reactivity in the OML (Figures 1F and 1G, 45 min after beginning HFS). These results clearly demonstrate that only the synaptic layers that had undergone LTP showed an increase in phalloidin reactivity. The three strong HFSs of MPP fibers [HFS (2400), HFS (500), and HFS (300)] induced equivalent degree of LTP persistence and increases in phalloidin reactivity. Consequently, HFSs of (300) or higher will be used interchangeably as strong HFSs in the following experiments.

We next measured the levels of the soluble monomeric actin (G-actin) and the insoluble filamentous polymerized actin (F-actin) in the MML following the induction of L-LTP via the MPP (Figure 2). MMLs were collected by means of the Laser Capture Microdissection technique (Simone et al., 2000) from dehydrated frozen sections of the brain dissected 3 hr after beginning HFS (2400) of the MPP (Figure 2A). The MML tissues were fractionated by a buffer containing 1% Triton X-100, and the soluble and insoluble materials were subjected to quantitative Western blot analysis (Figure 2B). The total actin levels (G-actin + F-actin) of the MMLs from the control and LTP sides did not differ significantly (Figure 2C, number of animals tested = 3). However, in the LTP side, the ratio (R) of F-actin (insoluble) to G-actin (soluble) was higher compared to that of the control side (Figure 2C, $R_{LTP}/R_{control} = 1.31 \pm 0.14$). Thus, the increase in phalloidin reactivity in the MML observed after LTP induction indeed reflects an increase in the F-actin content in the synaptic layer.

Induction of L-LTP Increases F-Actin Levels in Dendritic Spines

Dendritic spines are extremely enriched in actin molecules (Capani et al., 2001; Fifkova, 1985; Matus et al., 1982). Confirming this is that laser confocal microscopy on control MML and inner molecular layer (IML) stained with phalloidin revealed multiple punctate signals that indicates the F-actin in the spine (Figure 3A, left). When the MPP received HFS (2400), the intensity of the punctate signals in the MML were elevated without changing in the IML, which suggests that the F-actin in the dendritic spine increases after LTP induction (Figure 3A, right).

To investigate this phenomenon further, we examined MMLs by electron microscopy using a recently described high-resolution photoconversion method (Capani et al., 2001) to visualize the precise distribution of F-actin. Phalloidin conjugated to the fluorophore eosin was used to label F-actin. The oxygen radicals released by eosin excitation oxidize diaminobenzidine tetrahydrochloride (DAB), which then becomes electron-dense when it is treated with osmium. Figure 3B shows examples of electron micrographs taken of the MML 45 min after HFS (2400) had begun. The large and morphologically diverse dendritic spines (arrows) showed intense phalloidin reactivity throughout their spine cytoplasm and PSD, whereas the small and morphologically simple spines (arrowheads) showed intense phalloidin reactivity mainly at PSD. These observations confirm those of Capani et al. (2001). Electron micrographs of MML of the LTP side without photoconversion show weaker electron density in the PSD (Figure 3B, bottom), indicating that the dark PSD staining after photoconversion is indeed due to the presence of actin in the PSD.

We counted the MML synapses with intensely phalloidin-reactive spines. We defined intensely phalloidin-reactive spines as those whose phalloidin staining throughout their spine cytoplasm is stronger than in the

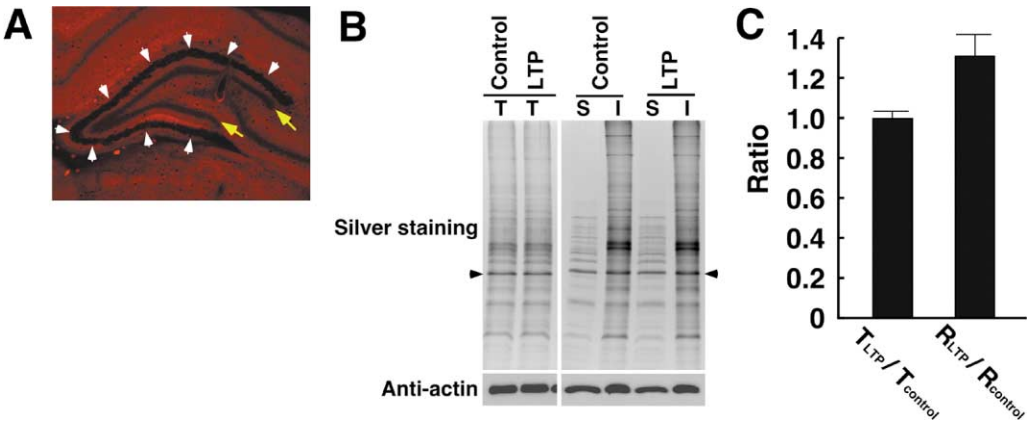

Figure 2. LTP Is Accompanied by a Net Enhancement of F-Actin Content in the Molecular Layer

(A) Brain was dissected 3 hr after HFS (2400) of the MPP fibers. MML was collected from the hippocampal section (30 μm thickness) with the Laser Capture Microdissection System LM2000. After the laser treatment, the section was stained with phalloidin-TRITC. The area corresponding to the MML (black zone) is indicated by white arrowheads. The yellow arrows show the GCL (dark zone).

(B) MML tissues from hippocampal sections dissected 3 hr after HFS (2400) of the MPP fibers were collected and fractionated. The total (T), soluble (S), and insoluble (I) materials were then separated by SDS-PAGE and silver-stained (top panel) or Western blotted with an anti-actin antibody (bottom panel). Silver-staining image demonstrates that all the proteins were prepared without any degradation. Arrowheads indicate a signal of actin molecule.

(C) The immunopositive signals on the Western blot were quantified by LAS-1000. T_{LTP}, total actin in the LTP side; $T_{control}$, total actin in the control side; R_{LTP} and $R_{control}$, ratio of insoluble actin to soluble actin in the LTP and control sides, respectively.

corresponding presynaptic terminal, and weakly phalloidin-reactive spines as those having equal or less staining in the spine cytoplasm than in the presynaptic terminal. Intensely phalloidin-reactive spines occurred significantly more frequently in the LTP side (64.3% ± 0.9%) than in the control side (31.5% ± 7.9%; *$p < 0.05$, Welch t test, number of slices = 3; synapse numbers examined, 975 for LTP side and 1199 for control side) (Figure 3C). However, the actual synaptic density in the MMLs of the control and LTP sides did not differ significantly (control versus LTP, 6.8 ± 0.63 versus 5.8 ± 0.74 synapses/10 μm^2) (Figure 3D). We further determined the length of the synaptic apposition in a total of 401 and 370 synapses in the MMLs of the control and LTP sides, respectively (Figure 3E). In the control side, the synaptic appositions of intensely phalloidin-reactive spines were markedly longer than that of the weakly phalloidin-reactive spines (weak versus intense, 170 ± 3.6 versus 347 ± 12.6 nm, $p < 0.05$, Welch t test). Essentially the same result was obtained with the LTP side (weak versus intense, 184 ± 8.2 versus 370 ± 9.5 nm, $p < 0.05$, Welch t test), except that there were significantly more synapses with an intensely phalloidin-reactive spine and a long synaptic apposition than in the control side, with complementary decrease in synapses with a small and weakly phalloidin-reactive spine (Figure 3E). Thus, 45 min after beginning HFS of MPP fibers, pre-existing spines show enhanced actin polymerization or suppressed depolymerization but there is no increase in synapse numbers. It remains to be determined whether the synapse numbers increase at later time points.

The Increase in F-Actin Is Dependent on NMDA Receptor Activation but not on De Novo Protein Synthesis

The induction of dentate gyrus LTP depends on NMDA receptor activation that occurs upon HFS (Errington et al., 1987). The prolonged maintenance of dentate gyrus LTP requires de novo protein synthesis that takes place around the time of HFS delivery (Abraham et al., 1993). We phalloidin-stained brain slices from rats injected with MK801, an NMDA receptor antagonist, that were then given HFS (500) and dissected 20 min later. We found that the HFS-induced increase in phalloidin reactivity was completely blocked by the MK801 treatment (Figure 4A). In contrast, preadministration of cycloheximide, an inhibitor of protein synthesis, did not alter the increase in phalloidin reactivity induced by HFS (500) (Figure 4A). Thus, the enhancement of F-actin content in the dendritic spine depends on NMDA receptor signaling, not on de novo protein synthesis.

The Increase in F-Actin Persists for Five Weeks and Correlates with LTP Persistence

When the phalloidin reactivity of the brain was examined 20 min, 24 hr, 1 week, and 5 weeks after HFS (500) of the MPP fibers, it was found that the elevated phalloidin reactivity in the MML was sustained at high levels for 1 week (Figure 4B). Elevated reactivity was also still observed at 5 weeks, although to a lesser extent. In contrast, although weak HFS (90) of MPP fibers also increased F-actin content in the MML at 45 min, the increase did not persist at 1 week (Figure 4C). This pattern correlates with the persistence of LTP, as LTP elicited by strong HFS (500) persists for 1 week, while LTP caused by weak HFS (90) has returned to basal levels at 1 week (Figure 1B). Thus, LTP persistence correlates with the duration that spine F-actin content is elevated.

Disruption of Actin Reorganization Impairs the Late Phase of LTP

To further investigate the role spine actin dynamics play in LTP, we examined whether actin dynamics inhibitors (ADIs) can modulate dentate gyrus LTP. To do this, we

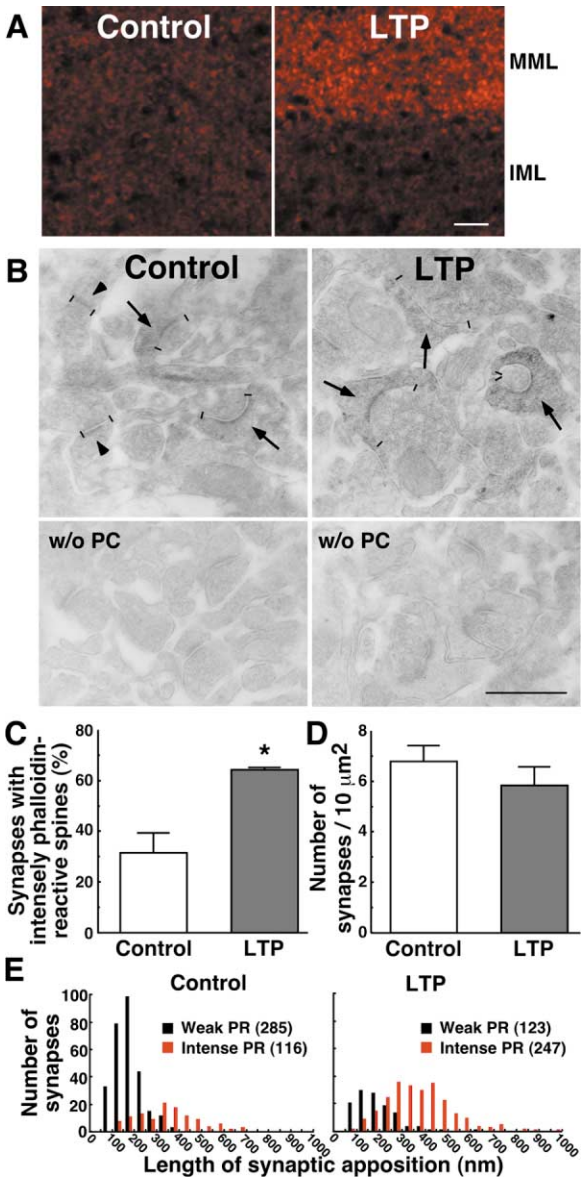

Figure 3. HFS of MPP Induces a Net Increase in the F-actin of the Dendritic Spines in the MML

(A) Confocal images of the phalloidin reactivity of the border between MML and IML. Left: unstimulated side. Right: MML/IML border dissected 45 min after beginning HFS (2400) of the MPP. The punctate signals may indicate the F-actin in the dendritic spines. The bar represents 5 μm.

(B) Typical electron micrographs showing phalloidin reactivity of the MML. The MPP was given HFS (2400) to elicit LTP in MML synapses, and 45 min after beginning HFS brain was subjected to electron microscopic analysis. Phalloidin reactivity was visualized by the photoconversion method. Top panels: electron micrographs were taken from areas that had been exposed to light (515 nm) from a mercury lamp. Note the intense signal throughout the spine cytoplasm in the large and morphologically diverse spines (arrows). The arrowheads indicate the small and morphologically simple spines. The length of pre- and postsynaptic apposition, which is sandwiched by small bars, was measured to evaluate morphological characteristics of each spine. Bottom panels: electron micrographs taken from MML areas outside of the light-exposed area (without photoconversion). The scale bar represents 500 nm. PC, photoconversion.

(C) The synapses with intensely phalloidin-reactive spine in three sections (100 μm apart) of the MML 45 min after the MPP had been given HFS (2400) were counted. A total of 1199 and 975 synapses in the MMLs of the control and LTP sides, respectively, were examined. *, $p < 0.05$, Welch t test, number of slices = 3.

(D) The synaptic density in the MML of the LTP side [45 min after the beginning of HFS (2400)] did not differ significantly from that of the control side. The number of synapses examined was same as in (C).

(E) Histograms showing the distribution of the length of synaptic apposition in the MML of the control and LTP [45 min after the beginning of HFS (2400)] sides. PR, phalloidin reactivity. Numbers in parentheses indicate number of synapses examined.

used urethane-anesthetized rats implanted with a recording electrode (stainless steel pipe electrode) linked to a syringe that can deliver various pharmacological agents to the dentate gyrus (see Experimental Procedures for details). We tested ADIs, a protein synthesis inhibitor, or vehicle alone (Figure 5). When we tested latrunculin A (50 μM), which sequesters G-actin and consequently causes F-actin depolymerization (Spector et al., 1989), or the protein synthesis inhibitor cycloheximide (10 mg/ml) on unstimulated rats, the basal synaptic transmission over 12 hr did not vary compared to the case when the vehicle was applied (Figure 5A).

With regards to LTP elicited by HFS (2000), when the recording electrode delivered cycloheximide, the LTP decayed to basal levels within 8 hr (Figure 5B, 103.6% ± 5.13% at 8 hr), indicating that E-LTP, which does not require de novo protein synthesis, decays within 8 hr in this LTP model. Importantly, latrunculin A blocked the development of late-phase LTP, as the LTP induced by HFS (2000) delivered 1 hr after administering the latrunculin A decayed 8 hr later to 98.9% ± 5.69% of the fEPSP slope obtained in the 60 min preceding HFS (Figure 5B). However, latrunculin A did not affect the initial amplitude and early maintenance of LTP, as at 30–50 min the LTP was 123% ± 4.7% of the fEPSP slope obtained in the 60 min preceding HFS. The difference in the HFS (2000)-evoked response by the control and latrunculin A groups became statistically significant at 8 hr ($p < 0.05$), and the decay of the LTP in the presence of latrunculin A resembled that of cycloheximide-treated LTP.

To exclude the possibility that latrunculin A does not affect LTP induction because it is inefficiently infused into the neurons at the time of HFS, the tube delivering latrunculin A was cut to promote drug infusion into the dentate gyrus and HFS was delivered 4 or 7.5 hr later (rather than 1 hr later) (Figure 5C). At both of these time points, the LTP amplitudes of the control and latrunculin A groups in the previous experiment differed. Infusion of latrunculin A even 7.5 hr prior to HFS had no effect on the initial LTP amplitude (control, 112.7% ± 2.36%; latrunculin A, 113.3% ± 3.07%, $p = 0.88$, Student's t test). Thus, the inhibition of actin assembly inhibits L-LTP without affecting E-LTP. These observations strongly suggest that a net increase in F-actin in the dendritic spine is important in the late phase of dentate gyrus LTP.

Another ADI, cytochalasin B, which caps the barbed end of F-actin and decreases F-actin levels (Cooper, 1987), did not significantly impair either the early or late phase of LTP at a dose of 50 μM (Figure 5D). Cytochalasin B at a higher dose (250 μM) partially impaired the

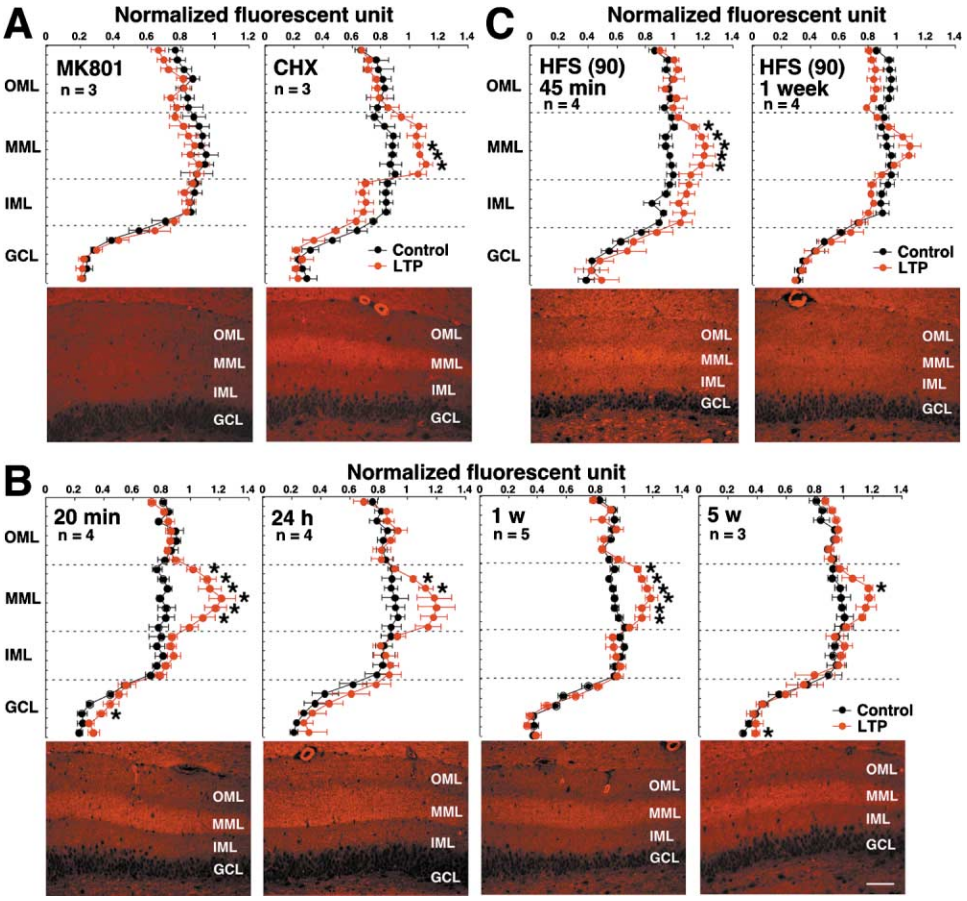

Figure 4. Effect of Pharmacological Agents on Actin Polymerization and Duration of Actin Polymerization

Phalloidin reactivity was quantified as in Figure 1G. LTP, ipsilateral LTP side; control, contralateral side. *, $p < 0.05$, compared with control side, t test. n, number of animals used for quantification.

(A) Phalloidin reactivity of brain slices of rats intraperitoneally injected with MK801, an NMDA receptor inhibitor (2 mg/kg body weight), or cycloheximide, a protein synthesis inhibitor (50 mg/kg body weight), given HFS (500) 45 min later and dissected after 20 min. CHX, cycloheximide.

(B) Time-dependent changes in the phalloidin reactivity of the molecular layer of the dentate gyrus after HFS (500) (20 min, 24 hr, 1 week, and 5 weeks). Scale bar equals 100 μm.

(C) F-actin levels in the MML following weak HFS (90).

late phase of LTP, although statistically not significant. This may be attributed to the fact that the F-actin within the dendritic spines of cultured hippocampal neurons is more resistant to the action of cytochalasin than to latrunculin A (Allison et al., 1998).

Importance of Actin-Depolymerizing Factor (ADF)/Cofilin in L-LTP

The turnover of actin filaments can be regulated by a number of actin binding proteins, including the ADF/cofilin family of proteins. These molecules have F-actin severing and F-actin depolymerizing activities and consequently stimulate actin filament turnover (for reviews, see Carlier and Pantaloni, 1997; Chen et al., 2000; Pantaloni et al., 2001). There is ample evidence that ADF/cofilin plays a pivotal role in regulating actin dynamics in the nervous system, as it is highly expressed in the nervous system (Bamburg and Bray, 1987) and its activity regulates process extinction and neurite outgrowth in cortical neurons (Meberg and Bamburg, 2000). Furthermore, its phosphorylation is believed to regulate the actin filament turnover that is thought to lead to growth cone collapse (Aizawa et al., 2001).

The F-actin depolymerizing activity of ADF/cofilin is negatively regulated by phosphorylation at a single site (Ser-3) (Agnew et al., 1995; Moriyama et al., 1996), and excessive actin polymerization is observed in mammalian and fly cells with highly phosphorylated ADF/cofilin (Arber et al., 1998; Niwa et al., 2002; Toshima et al., 2001; Yang et al., 1998). We therefore asked whether the level of ADF/cofilin phosphorylation in the dentate gyrus changes after L-LTP is induced (Figure 6). Because anti-phospho (Ser-3)-ADF/cofilin antibody used in this study was not suitable for immunohistochemistry, we carried out immunoblot to examine the change in the phosphorylation level. MMLs with and without HFS (500) were collected using the Laser Microdissection System LMD (Figure 6A) and subjected to quantitative Western blot analysis with anti-phospho (Ser-3)-ADF/cofilin antibody. This revealed that HFS (500) of the MPP fibers significantly increased the phosphorylation of Ser-3 of ADF/cofilin (Figures 6B and 6C). This increase

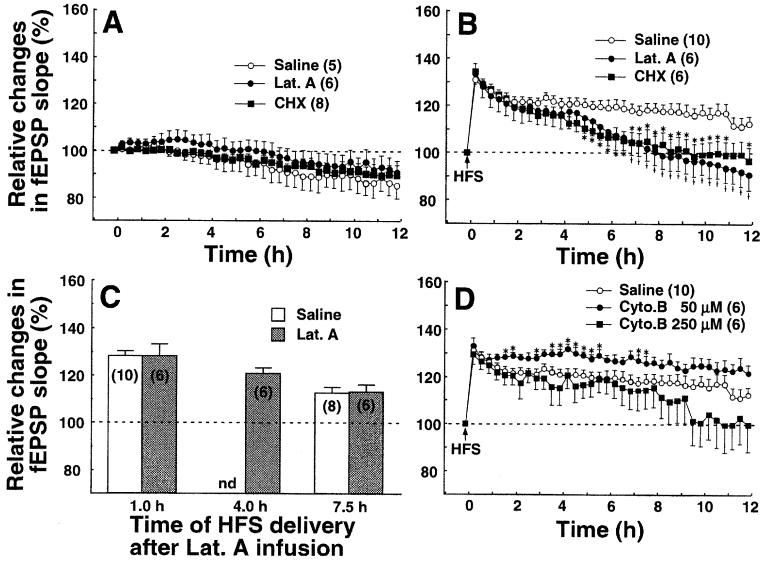

Figure 5. Inhibition of Actin Reorganization Specifically Blocks the Late Phase of LTP

All the LTP experiments in this figure were performed with urethane-anesthetized rats.

(A) Effect of latrunculin A (50 μM, closed circle), cycloheximide (10 mg/ml, closed square), and vehicle (saline containing 0.1% DMSO, open circle) on basal synaptic transmission. The polyethylene tube delivering the drug was cut at time −0.5 hr to promote infusion of the solution into the tissue. The average of the fEPSP slope during the 60 min prior to time 0 served as the baseline (100%).

(B) Effect of latrunculin A (50 μM, closed circle) and cycloheximide (10 mg/ml, closed square) on LTP persistence. HFS (2000) was delivered at time 0. The polyethylene tube was cut 1 hr before HFS (2000). A faster LTP decay was observed both in the latrunculin A group [versus DMSO group, $F(1,14) = 5.124$, $p < 0.05$] and the cycloheximide group [versus DMSO group, $F(1,14) = 6.009$, $p < 0.05$]. An asterisk indicates a statistically significant difference between the DMSO and cycloheximide groups, while a dagger indicates a statistically significant difference between the DMSO and latrunculin A groups.

(C) Latrunculin A specifically inhibits the late phase of LTP without affecting LTP induction. HFS (2000) was delivered 1, 4, or 7.5 hr after cutting the tube delivering latrunculin A. The relative change in the fEPSP slope 30 min after the HFS delivery is shown.

(D) Effect of cytochalasin B on LTP persistence. HFS (2000) was delivered 1 hr after cutting the tube delivering cytochalasin B. Cytochalasin B had no significant effect on LTP (saline versus Cyto. B 50, $p > 0.05$; saline versus Cyto. B 250, $p > 0.05$, Student's t test).

Numbers in parentheses indicate the number of animals used. Abbreviations: Lat. A, latrunculin A; CHX, cycloheximide; Cyto. B, cytochalasin B; nd, not determined.

was observed at 30 min and persisted for at least 5 hr. This strongly suggests that the net increase in F-actin levels during L-LTP is caused and maintained, at least in part, by a decrease in the actin-depolymerizing activity of ADF/cofilin.

If the net enhancement of F-actin content in the dendritic spine during L-LTP is mediated by a downregulation of the ADF/cofilin activity, then we can expect that inhibiting ADF/cofilin phosphorylation would affect L-LTP. To assess this, we synthesized a hybrid peptide comprised of a unique sequence consisting of the phosphorylation site of ADF/cofilin (S3-peptide) that would act as a competitive inhibitor for ADF/cofilin phosphorylation (Aizawa et al., 2001), and a stretch of arginines (11R) that would ensure the efficient delivery of the peptide into the hippocampal neurons (Matsushita et al., 2001). A control peptide was also synthesized that has the reverse sequence of the S3-peptide followed by 11R. These synthetic peptides were indeed efficiently incorporated into the granule cells of the dentate gyrus when delivered through the recording electrode (Figure 6D). In the urethane-anesthetized rats, strong HFS (2000) in the presence of the control peptide (Rev-11R) elicited L-LTP in the dentate gyrus that lasted at least 12 hr (Figure 6E). Control peptides (150 ng/μl and 300 ng/μl) had no significant effect on LTP (saline versus Rev-11R, $p > 0.05$). In contrast, while injection of the inhibiting peptide S3-11R (150 ng/μl) had no effect on the induction and early maintenance of dentate gyrus LTP, it partially affected the late phase of LTP (Figure 6E, left, S3-11R). That is, the LTP amplitude observed in the inhibiting peptide group was similar to that of the control peptide group until 6 hr after HFS (2000), at which point it steadily declined to reach a plateau of about 105% of the baseline. In the animals infused with a higher concentration of the S3-11R peptide (300 ng/μl), the LTP decayed even more rapidly compared to the control animals without affecting the initial LTP amplitude (Figure 6E, right).

Immunoreactivities to Actin-Associated Proteins Increase in the MML after LTP Induction

That LTP induction causes a net enhancement of F-actin content in the dendritic spine suggests that LTP induction is accompanied by a change in the molecular composition of the dendritic spine. We tested this by examining the MML after HFS (300) for immunoreactivities against drebrin and synaptopodin, two actin-associated proteins known to localize in the dendritic spine (Figure 7). While both proteins were equally distributed throughout the molecular layer of the control dentate gyrus, 45 min after delivering HFS (300) to the MMP, an intense immunoreactivity that localized specifically to the MML was observed (Figure 7A). This staining pattern is almost identical to that of phalloidin and persisted partially for 3 weeks (Figure 7B, $n = 5$). Thus, the actin-based molecular composition of the activated dendritic spines alters after LTP is induced. This change may cause a dynamic rearrangement of functional synaptic proteins such as receptors and signaling molecules and could further trigger a morphological change in the dendritic spine, which are two events that appear to be important for the maintenance of L-LTP.

In contrast to the actin-associated proteins, the LTP and control hippocampal sections do not appear to differ in their immunoreactivities against microtubule-associated protein-2 (MAP-2) and neuron-specific β-tubulin (isotype 6) (Figure 7A, at 45 min). Both MAP-2 and β-tubulin, which are important in neuronal functions, are components of the tubulin cytoskeleton. Taken together, these

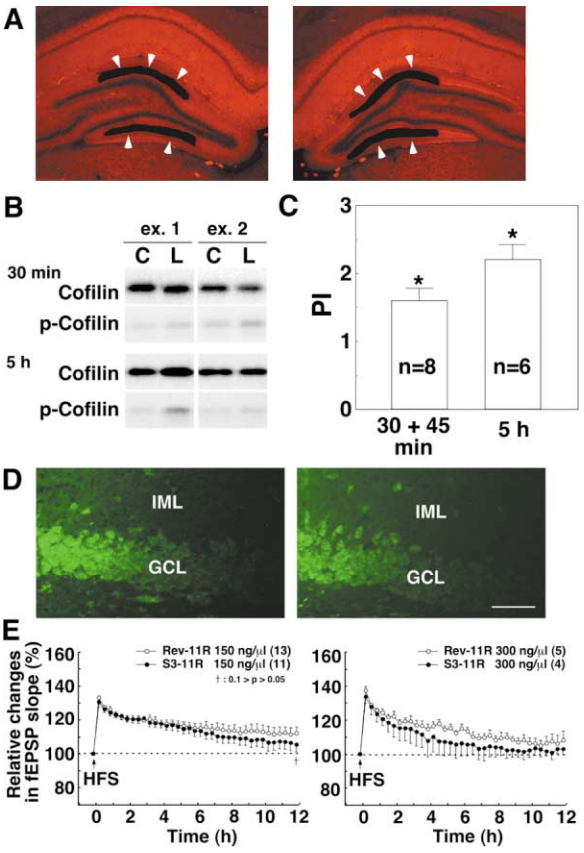

Figure 6. Involvement of ADF/Cofilin in Hippocampal LTP

(A) Representative images of the phalloidin staining of hippocampal sections obtained after collecting the MML tissues using the Laser Microdissection System (LMD). Arrows indicate the areas collected. Left, control side; right, LTP side.

(B) ADF/cofilin and phospho-ADF/cofilin (p-cofilin) antibody staining in Western blots of MML from frozen sections of brains that had been removed 30 min or 5 hr after HFS (500). Two representative examples for each time point are shown. C, control side; L, LTP side.

(C) Quantification of immunoblots were carried out for signal intensity to yield the phosphorylation index of ADF/cofilin. The phosphorylation index (PI) was calculated as follows: $PI = (pAC_{LTP}/AC_{LTP})/(pAC_{control}/AC_{control})$, where pAC and AC are signal intensities of phospho-ADF/cofilin and ADF/cofilin, respectively. Data from the 30 min ($n = 4$) and 45 min ($n = 4$) brains were combined. *, $p < 0.01$; one sample t test against hypothetical mean = 1.0. n, number of animals tested.

(D) FITC-labeled S3-11R peptide (left) or FITC-labeled Rev-11R peptide (right) was injected into the dentate gyrus of urethane-anesthetized rat through the recording electrode, and a hippocampal section was made 4 hr later to visualize the FITC fluorescence in the GCL. Position of the electrode is just left outside of each picture. GCL, granule cell layer; IML, inner molecular layer. Scale bar equals 100 μm.

(E) Effect of S3-11R and Rev-11R peptide on dentate gyrus LTP of urethane-anesthetized rats. HFS (2000) was delivered 1 hr after cutting the tube to administer the peptides. Numbers in parentheses indicate the number of animals used.

Note that the LTP experiments in (A)–(C) were carried out with unanesthetized rats, while the LTP in (E) was performed with urethane-anesthetized rats.

observations suggest that LTP induction is specifically accompanied by a change in the actin cytoskeleton and its associated proteins in the activated synaptic layer.

Discussion

Spine Actin Reorganization Is Critical for the Maintenance of LTP

In this study, we found that dentate gyrus LTP induction is associated with actin cytoskeletal reorganization characterized by a net increase in F-actin content in the dendritic spines. The increase is rapid, being observed as early as 20 min after stimulation, and is then sustained for at least 5 weeks. Since the synapse number has not changed 45 min after the L-LTP induction, the HFS-dependent increase in phalloidin reactivity observed at 45 min must reflect an increase in the amounts of F-actin in each spine. Intensely phalloidin-reactive spines have longer synaptic appositions than weakly phalloidin-reactive spines in both LTP and control sides. Furthermore, the ratio of intensely phalloidin-reactive spines versus weakly phalloidin-reactive spines is higher in the LTP side than in the control side. These observations suggest that a spine actin reorganization triggered by HFS results in morphological changes of the spine shape. This is consistent with a previous observation that HFS enlarges the PSD area of polyribosome-containing spines in the hippocampal CA1 region (Ostroff et al., 2002). Whether the increased phalloidin reactivity observed at later time points, for example at 24 hr, is due to the formation of new spines still has to be investigated.

When actin polymerization is inhibited by latrunculin A treatment, the initial amplitude and the early maintenance of LTP are not affected but the late phase of LTP is completely inhibited, indicating that the late phase is dependent on the restructuring of the actin cytoskeleton. The abundance of F-actin in the dendritic spines may, therefore, be a structural indicator for the ability of the synapses to maintain a change in synaptic efficacy. Supporting this is that in contrast to latrunculin A, cytochalasin B did not significantly affect the late phase of LTP. Cytochalasin effectively disrupts the F-actin within the soma and the dendritic shaft but not the F-actin within the spine (Allison et al., 1998). Importantly, we found a strong correlation between LTP persistence and the duration of F-actin augmentation. This may indicate that the increase of F-actin content in the pre-existing spines and the subsequent enlargement of spine morphology are critical for the late phase of LTP. Alternatively, at later time points, such as at 24 hr, formation of new spines (Trachtenberg et al., 2002) occurs and this contributes to the enhancement of phalloidin reactivity as well as the late maintenance of LTP.

That latrunculin A and the protein synthesis inhibitor cycloheximide both have equivalent effects in that they block the late phase of LTP, yet the accumulation of F-actin is not dependent on protein synthesis, suggests that the actin cytoskeleton is important for the functioning of newly synthesized proteins that are necessary for the late phase of LTP. Experiments with hippocampal CA1 slices have shown that the application of ADIs inhibit the pre- and postsynaptic functions needed for glutamatergic transmission and plasticity. These effects are dependent on the ADI drug concentration, as the postsynaptic function is more sensitive to ADIs (Kim and Lisman, 1999; Krucker et al., 2000). Consistent with our observations, a low dose of ADIs specifically inhibits

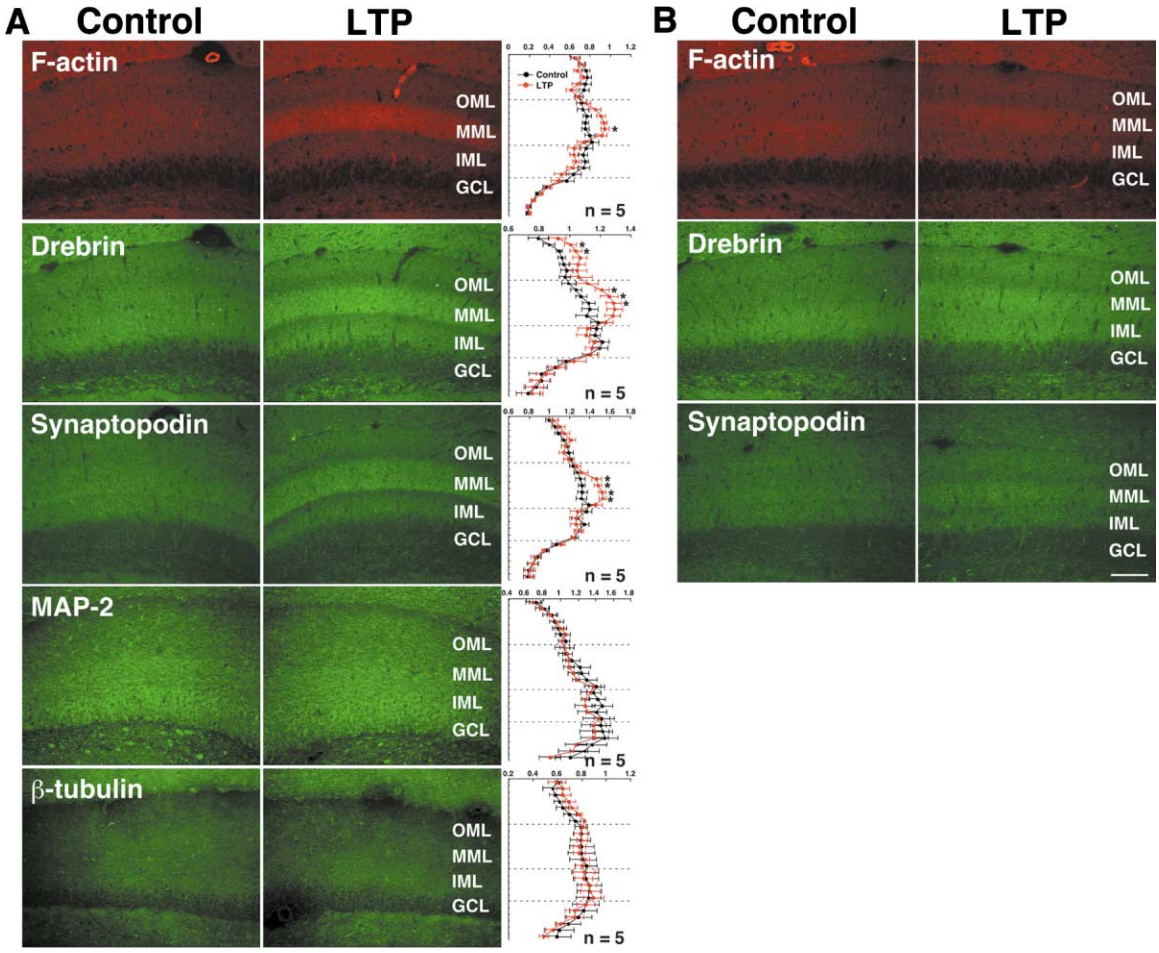

Figure 7. HFS of the MPP Specifically Alters Immunoreactivities of Postsynaptic Actin-Associated Proteins in the MML

The distributions of drebrin, synaptopodin, MAP-2, and neuron-specific class III β-tubulin were examined by immunohistochemistry 45 min (A) and 3 weeks (B) after HFS (300) of the MPP. Quantification of phalloidin reactivity was carried out as in Figure 1G. *, $p < 0.05$, compared with control side, t test. n, number of animals used for quantification. Scale bar equals 100 μm.

the maintenance phase of LTP of AMPAR component without affecting the induction (Krucker et al., 2000). It should be noted that our observations do not necessarily exclude the possibility that L-LTP has a more strict requirement for actin cytoskeletal reorganization than E-LTP.

Potential Mechanisms by which Reorganized Spine Actin Cytoskeleton Promotes the Late Phase of LTP

How can the reorganized spine actin cytoskeleton participate in the molecular mechanisms underlying the late phase of hippocampal LTP? The actin cytoskeleton plays multiple roles in a wide variety of cellular functions, including membrane trafficking, local protein trafficking, acting as a protein-anchoring scaffold, and establishing cell morphology (for reviews, see Halpain, 2000; Langford and Molyneaux, 1998; Matus, 2000; Schafer, 2002). The actin filaments in the dendritic spines may thus contribute to the late phase of LTP through several mechanisms.

First, they could facilitate a morphological change in the dendritic spine that supports L-LTP maintenance. It is known that prolonged changes in synaptic efficacy are accompanied by a structural remodeling of the dendritic spines, including the formation of multiple synaptic boutons and the sprouting of the postsynaptic architecture toward the presynaptic terminal (Buchs and Muller, 1996; Colicos et al., 2001; Geinisman et al., 1996; Toni et al., 1999; Trommald et al., 1996; Weeks et al., 1998). Since pharmacological and genetic perturbation of actin dynamics affects spine structures (Meng et al., 2002; Nakayama et al., 2000; Pak et al., 2001; Penzes et al., 2001; Tashiro et al., 2000), the actin cytoskeleton is the most likely target that regulates spine morphology. Spine morphology is tightly correlated with the distribution of AMPARs within the spines (Matsuzaki et al., 2001), indicating that actin-based morphogenetic regulation of the dendritic spines is critical to the synaptic efficacy. Thus, net enhancement of F-actin content may be coupled to a change in the spine morphology, thereby modulating the LTP persistence. Alternatively, the increase in F-actin reflects the stable postsynaptic actin sprouting that follows multiple tetanic stimuli (Colicos et al., 2001), which may contribute to L-LTP persistence through the formation of new synapses.

Second, the actin filaments in the dendritic spines may support membrane trafficking. A large number of recent studies have provided strong evidence that the insertion of AMPARs into the synaptic membrane and the internalization of the AMPARs from the synaptic membrane are both important in determining synaptic efficacy, as the insertion and internalization of AMPARs mediate LTP and long-term depression (LTD), respectively (Carroll et al., 2001; Hayashi et al., 2000; Lledo et al., 1998; Sheng et al., 2001; Shi et al., 1999, 2001). Both of these events are mediated by membrane trafficking since the receptors are inserted and removed from the synaptic membrane by the endocytosis and exocytosis, respectively, of AMPAR-containing vesicles. The actin cytoskeleton is involved in several distinct processes of both endocytosis and exocytosis (Cremona and De Camilli, 2001; Qualmann et al., 2000; Schafer, 2002). Supporting this is that when F-actin is disrupted by latrunculin A, AMPAR is internalized (Zhou et al., 2001). Furthermore, AMPAR internalization is blocked by jasplakinolide, an F-actin-stabilizing reagent (Zhou et al., 2001). Thus, the stabilization of the F-actin in the spines following LTP induction that we observed in this study may increase synaptic efficacy by blocking AMPAR endocytosis.

Third, the actin filaments in the dendritic spines may also support local protein trafficking. Gene expression and protein synthesis are necessary for L-LTP. Some of the proteins synthesized in the soma in response to a synaptic input, such as Vesl-1S/Homer-1a, synaptopodin, and arcadlin (Brakeman et al., 1997; Kato et al., 1997; Yamagata et al., 1999; Yamazaki et al., 2001), must be transported to the postsynaptic membrane or PSD to exert their function in L-LTP. Indeed, we found an increase in synaptopodin immunoreactivity of the synaptic layer after LTP is induced. F-actin is the sole cytoskeleton present in the dendritic spines and thus it must constitute the track that delivers these proteins from the dendritic shaft to the postsynaptic site through the spine cytoplasm. The subsequent fusion of membrane proteins with the postsynaptic membrane occurs by exocytosis and therefore also depends on the actin cytoskeleton. Thus, the actin cytoskeleton plays an essential role in the delivery of the appropriate postsynaptic proteins.

Fourth, the actin filaments may also act as a scaffold on which proteins are anchored. The F-actin in dendritic spines anchors macromolecular complexes (Allison et al., 1998; Halpain, 2000; van Rossum and Hanisch, 1999; Ziff, 1997). Plasticity-dependent changes in actin dynamics could alter the arrangement and functional state of postsynaptic proteins, including neurotransmitter receptors, signaling molecules, and scaffold proteins, thereby modulating the synaptic plasticity. Indeed, a critical role for PSD F-actin is implicated in the anchoring of AMPARs at postsynaptic sites during LTP (Lisman and Zhabotinsky, 2001). Moreover, actin dynamics are suggested to be involved in LTD mechanism, where deanchoring of the AKAP-PKA complex from the PSD associated with F-actin remodeling triggers the endocytosis of AMPARs (Gomez et al., 2002).

Signaling Mechanism Regulating Spine Actin Dynamics

Little is known about the molecular mechanisms that regulate actin reorganization in the dendritic spine, but our results demonstrate that ADF/cofilin is involved in regulating the actin dynamics during LTP. ADF/cofilin has F-actin severing and F-actin depolymerizing activity and consequently stimulates actin filament turnover (Carlier and Pantaloni, 1997; Chen et al., 2000; Pantaloni et al., 2001). We found that a strong HFS that elicits L-LTP enhances the phosphorylation of ADF/cofilin at its Ser-3 residue in the molecular layer, indicating that the activity of ADF/cofilin is suppressed by LTP-inducing stimuli. Furthermore, when the ADF/cofilin phosphorylation, which deactivates the molecule, was inhibited, the late phase of LTP was partially impaired.

What could be the signaling pathway that regulates the ADF/cofilin activity within the dendritic spine? One candidate could be the Rho family of small GTPases, which is known to be a key regulator of actin cytoskeleton dynamics in a variety of cell types (for a review, see Bishop and Hall, 2000). Rac and Rho, two members of this family, are implicated in spine shape changes in that the signaling pathway involving Rac promotes the formation and maintenance of the spine structure while the Rho pathway promotes spine retraction and prevents spine formation (Nakayama et al., 2000; Tashiro et al., 2000). Both of these pathways, which lead to an altered actin cytoskeleton, involve ADF/cofilin phosphorylation downstream of Rho and Rac activity. Both the Rac and Rho GTPases activate LIM kinase (LIMK) through the serine/threonine kinases Pak1 and ROCK (Roc), respectively (Edwards et al., 1999; Maekawa et al., 1999), and LIMK then in turn downregulates ADF/cofilin activity by phosphorylating Ser-3 (Arber et al., 1998; Yang et al., 1998). Thus, it may be that the Rac and Rho pathways could regulate the spine morphological changes supporting L-LTP by phosphorylating the downstream effector ADF/cofilin, which blocks its actin depolymerizing activity. Supporting this is a recent study with LIMK-1 knockout mice which revealed that LIMK-1 plays a crucial role in spine morphogenesis (Meng et al., 2002). The accumulation of F-actin in the dendritic spine was much lower in LIMK-1 knockout mice than in wild-type mice, and an abnormal spine morphology characterized by thicker necks and smaller heads was observed. However, as the inhibition of ADF/cofilin phosphorylation does not suppress L-LTP completely, it is possible that other regulators of actin organization, such as WASP and Arp, which promote actin polymerization, may also be involved in regulating the organization of spine actin during LTP.

Experimental Procedures

Animals

All procedures involving the use of animals complied with the guidelines of the National Institute of Health and were approved by the Animal Care and Use Committee of Mitsubishi Kagaku Institute of Life Sciences. Male Wistar ST rats approximately 20 weeks of age were used for LTP experiments.

Reagents and Antibodies

All reagents used in this study were purchased from Nacalai Tesque (Kyoto, Japan) unless otherwise indicated. The phalloidin-eosin con-

jugate and latrunculin A were from Molecular Probes (Oregon), and bovine serum albumin (BSA), phalloidin-tetramethylrhodamine B isothiocyanate (TRITC) conjugate, and cycloheximide (CHX) were from Sigma Chemical (Missouri). Mouse anti-MAP2 monoclonal antibody and FITC-conjugated goat anti-mouse and anti-rabbit secondary antibodies were from Chemicon (California), while rhodamine-conjugated goat anti-mouse IgM secondary antibody was purchased from ICN (California). The mouse monoclonal anti-cofilin antibody (MAB-22) (Abe et al., 1989) and the rabbit anti-neuron-specific class III β-tubulin (Mβ6) antibody (Takiguchi et al., 1998) were kindly donated by Dr. T. Obinata at the Chiba University and Dr. Y. Arimatsu at the Mitsubishi Kagaku Institute of Life Sciences, respectively. The fluorescein (FITC)-labeled S3-11R peptide (HMASGVAVSDGVIKVFN MRRRRRRRRRRRK-FITC) and the reverse S3-11R peptide (Rev-11R, HNFVKIVGDSVAVGSAMMRRRRRRRRRRRK-FITC) were synthesized by Multiple Peptide Systems (California).

Dentate Gyrus LTP in Unanesthetized Freely Moving Animals

We used the surgical procedure described previously (Kato et al., 1997, 1998) with a slight modification. Briefly, a bipolar stimulating electrode and a monopolar recording electrode made of tungsten wire were positioned stereotaxically so as to selectively stimulate MPP and LPP projections while recording in the dentate gyrus. The electrode stimulating the MPP fibers was positioned 8.7 mm posterior, 5.3 mm lateral, and 5.3 mm inferior to the bregma. The electrode stimulating the LPP fibers was positioned 7.4 mm posterior, 5.9 mm lateral, and 7.0 mm inferior to the bregma. A recording electrode was implanted ipsilaterally 4.0 mm posterior, 2.5 mm lateral, and 3.8 mm inferior to the bregma. Rats were allowed to recover for at least 2 weeks in individual home cages.

LTP experiments on freely moving and unanesthetized animals were performed as described previously (Matsuo et al., 2000) with the following modifications. We used three strong tetanic stimuli (biphasic square wave form, 200 μs pulse width), namely HFS (2400), HFS (500), and HFS (300), all of which elicit long-lasting L-LTP (numbers in parentheses indicate total stimulation pulses) (Figure 1B). HFS (2400) consisted of four trains with 15 min intertrain intervals. Each train consisted of 20 bursts of 30 pulses at 400 Hz, delivered at 5 s interburst intervals. HFS (500) and HFS (300) consisted of ten and six trains with 1 min intertrain intervals, respectively. Each train consisted of five bursts of ten pulses at 400 Hz, delivered at 1 s interburst intervals. The weak tetanic stimulation HFS (90) consisted of six trains at 10 s intertrain intervals. Each train consisted of 15 pulses at 200 Hz (biphasic square wave form, 200 μs pulse width). In some experiments, animals were injected intraperitoneally 45 min prior to the beginning of HFS (500) with the NMDA receptor inhibitor dizocilpine maleate (MK801; 2 mg/kg body weight) or the protein synthesis inhibitor cycloheximide (50 mg/kg body weight).

Dentate Gyrus LTP in Urethane-Anesthetized Animals and Drug Delivery

LTP experiments with urethane-anesthetized rats were carried out as described previously (Inokuchi et al., 1996; Matsuo et al., 1998) with the following modifications. A bipolar tungsten electrode was used for stimulation and a stainless steel pipe electrode (i.d., 80 μm; o.d., 200 μm) for recording and drug delivery. The recording electrode was connected to a microsyringe via a polyethylene tube. Before implantation, the recording electrode was filled with either latrunculin A, cytochalasin B, cycloheximide, synthetic peptide, or the vehicle solution (saline containing 0.1% or 0.5% DMSO). The stimulating electrode (8.0 mm posterior, 4.5 mm lateral, and 5.0 mm inferior to the bregma) and the recording electrode (4.0 mm posterior, 2.5 mm lateral, and 3.8 mm inferior to the bregma) were implanted unilaterally after the animal had been anesthetized by urethane (i.p., 1.0 g/kg body weight). All the stimuli were biphasic square wave pulses (200 μs width), and their intensities were set at the current that evoked 40% of the maximum population spike amplitude. After monitoring a stable basal transmission for at least 30 min, the polyethylene tube that connected the recording electrode to the microsyringe was cut to promote infusion of drug solution into the dentate gyrus through the tip of the recording electrode (Steward et al., 1998). This usually occurred 3–4 hr after the electrode implantation. The baseline synaptic transmission was further monitored for 1, 4, or 7.5 hr, after which the HFS was delivered. LTP was induced by HFS (2000), which consisted of five trains at 2 min intertrain intervals. Each train consisted of 400 pulses at 400 Hz. Test stimuli were delivered at 40 s intervals to monitor fEPSP. The body temperature of the animals was kept at 37°C throughout the LTP experiments by the Animal Blanket System MK-900 (Muromachi Kikai Co., Tokyo, Japan).

Histochemistry

Rats were sacrificed under anesthesia and the brain was immediately removed, frozen in dry ice, and then cut coronally with a cryostat microtome at 10 μm thickness. Sections were fixed for 30 min in 50 mM phosphate-buffered saline (PBS) containing 4% paraformaldehyde, treated with PBS containing 0.1% Triton X-100, incubated with PBS containing 2.5% BSA and 2.5% whole goat serum (ICN Biochemicals, Ohio), and then incubated overnight at 4°C with phalloidin-TRITC (0.1 ng/ml), FITC-DNase I (9 μg/ml), or a primary antibody against actin (10 μg/ml), synaptopodin (Progen, Heidelberg, Germany), drebrin (1 μg/ml; MBL, Nagoya, Japan), MAP2 (1/100), or β-tubulin (1/500). After several washes with PBS, sections were incubated with a secondary antibody (FITC- or rhodamine-conjugated anti-rabbit or anti-mouse antibody, Chemicon, 1/200 dilution). Fluorescent images were acquired either by a cooled 3CCD camera (Hamamatsu Photonics, Shizuoka, Japan) with MacScope software (Mitani Co., Tokyo, Japan) or by a laser-scanning confocal microscope LSM 5 PASCAL (Carl Zeiss, Jena, Germany). Fluorescence intensity was measured using the MacScope software and all the image preparations were performed by Photoshop software (Adobe, California).

Electron Microscopy by the Fluorescence Photooxidation Method

Observation of phalloidin reactivity by electron microscopy was performed using a procedure based on a previously described method (Capani et al., 2001). Briefly, rats were deeply anesthetized with pentobarbital and fixed by cardiac perfusion with 150 ml of PLP fixative (0.01 M $NaIO_4$, 0.75 M lysine, 2% paraformaldehyde). The brain was removed, immersed in PBS containing 20% sucrose, and then frozen in dry ice. Cryo-sections (20 μm) were immersed in PBS containing 0.1% Triton X-100, treated with PBS containing 0.05 M glycine and 0.5% cold-water fish gelatin (PBSGG), and then each section was incubated overnight at 4°C with 10 U eosin-phalloidin (Molecular Probes, Inc., Oregon) in 100 μl of PBSGG. Sections were then exposed to light (515 nm) from a mercury lamp for 30 min in 0.1 M sodium cacodilate buffer containing 2.8 mM DAB under continuous O_2 bubbling, and then post-fixed with 1% osmium. After dehydration and embedding in resin, ultrathin sections were cut on a Poter-Blum MT2-B ultramicrotome and examined with a Hitachi H-600A electron microscope.

Actin Analysis

Three rats were sacrificed 3 hr after the delivery of HFS (2400). Ten cryo-sections (coronal cut at 30 μm thickness) from each animal were fixed with 70% ethanol for 90 s, dehydrated with ethanol, immersed in xylene, and then air-dried. The MMLs were dissected and collected using the Laser Capture Microdissection System (LM2000, Arcturus Eng. Inc., California) (Simone et al., 2000). F-actin and G-actin were separated as described (Patterson et al., 1999). Briefly, ten dissected tissues were lysed in 50 μl lysis buffer (1% Triton X-100, 20 mM HEPES-HCl [pH 7.2], 100 mM NaCl, 1 mM Pefabloc) for 3 hr and the lysate was then subjected to centrifugation at 10,000 × g for 20 min. Ten microliter aliquots of the G-actin fraction (supernatant) and the F-actin fraction (pellet, dissolved in 50 μl SDS sample buffer) were subjected to SDS-PAGE (10% polyacrylamide). Western blot analysis was performed with the anti-actin antibody and the immunopositive signals were visualized and quantified by LAS-1000 Plus Luminescent Image Analyzer (Fujifilm, Tokyo, Japan).

Analysis of Phospho-ADF/Cofilin

Rats were sacrificed 30–45 min or 5 hr after the delivery of HFS (500). Ten cryo-sections from each animal (coronal cut at 20 μm

thickness) were air-dried, and the MMLs of each side of the dentate gyrus were dissected and collected separately using the Laser Microdissection System (LMD; Leica Microsystems, Wetzlar GmbH, Germany). The collected tissue was treated with 100 μl of SDS sample buffer (2% SDS, 100 mM Tris-HCl [pH 6.8], 33 mM NaCl, 1 mM EDTA, 40 mM DTT, 0.01% BPB, 10% glycerol) to extract proteins. One-fifth of each extract (20 μl) was subjected to SDS-PAGE (12% polyacrylamide) and transferred to a PVDF membrane (Millipore, Massachusetts) followed by immunodetection with anti-phospho (Ser-3)-ADF/cofilin antibody (Toshima et al., 2001). After the complete stripping of primary and secondary antibodies by treating the membrane with antibody-stripping solution (100 mM 2-mercaptoethanol, 2% SDS, 62.5 mM Tris-HCl [pH 6.7]) for 30 min at 50°C, the same membrane was reblotted with anti-cofilin antibody (MAB-22) to detect cofilin. The immunopositive signals were visualized and quantified by the LAS-1000 Plus Luminescent Image Analyzer.

Data Analysis

Data were expressed as means ± standard error and statistically analyzed with InStat 3 software (GraphPad software, California) and Statview software (Abacus Concept Inc., California).

Acknowledgments

We thank Drs. T. Obinata (Chiba University) and Y. Arimatsu (MITILS) for the monoclonal mouse anti-cofilin antibody and the rabbit anti-neuron-specific β-tubulin antibody, respectively, and K. Ohashi, M. Takahashi, H. Ohnishi, and S. Ono for their helpful discussions. We also thank A. Murayama for technical assistance. This work was performed through Special Coordinate Funds for Promoting Science and Technology from the Ministry of Education, Culture, Sports, Science, and Technology of the Japanese Government. This work was supported in part by Grant-in-Aid for Scientific Research (no. 14780610) to Y.F. and by grants for Scientific Research on Priority Areas (A)-Neural Circuit Project and (C)-Advanced Brain Science Project to K.I. from the Ministry of Education, Culture, Sports, Science, and Technology of the Japanese Government.

Received: September 10, 2002
Revised: March 11, 2003
Accepted: March 20, 2003
Published: May 7, 2003

References

Abe, H., Ohshima, S., and Obinata, T. (1989). A cofilin-like protein is involved in the regulation of actin assembly in developing skeletal muscle. J. Biochem. (Tokyo) *106*, 696–702.

Abraham, W.C., Mason, S.E., Demmer, J., Williams, J.M., Richardson, C.L., Tate, W.P., Lawlor, P.A., and Dragunow, M. (1993). Correlations between immediate early gene induction and the persistence of long-term potentiation. Neuroscience *56*, 717–727.

Agnew, B.J., Minamide, L.S., and Bamburg, J.R. (1995). Reactivation of phosphorylated actin depolymerizing factor and identification of the regulatory site. J. Biol. Chem. *270*, 17582–17587.

Aizawa, H., Wakatsuki, S., Ishii, A., Moriyama, K., Sasaki, Y., Ohashi, K., Sekine-Aizawa, Y., Sehara-Fujisawa, A., Mizuno, K., Goshima, Y., and Yahara, I. (2001). Phosphorylation of cofilin by LIM-kinase is necessary for semaphorin 3A-induced growth cone collapse. Nat. Neurosci. *4*, 367–373.

Allison, D.W., Gelfand, V.I., Spector, I., and Craig, A.M. (1998). Role of actin in anchoring postsynaptic receptors in cultured hippocampal neurons: differential attachment of NMDA versus AMPA receptors. J. Neurosci. *18*, 2423–2436.

Arber, S., Barbayannis, F.A., Hanser, H., Schneider, C., Stanyon, C.A., Bernard, O., and Caroni, P. (1998). Regulation of actin dynamics through phosphorylation of cofilin by LIM-kinase. Nature *393*, 805–809.

Bailey, C.H., Bartsch, D., and Kandel, E.R. (1996). Toward a molecular definition of long-term memory storage. Proc. Natl. Acad. Sci. USA *93*, 13445–13452.

Bamburg, J.R., and Bray, D. (1987). Distribution and cellular localization of actin depolymerizing factor. J. Cell Biol. *105*, 2817–2825.

Bishop, A.L., and Hall, A. (2000). Rho GTPases and their effector proteins. Biochem. J. *348*, 241–255.

Brakeman, P.R., Lanahan, A.A., O'Brien, R., Roche, K., Barnes, C.A., Huganir, R.L., and Worley, P.F. (1997). Homer: a protein that selectively binds metabotropic glutamate receptors. Nature *386*, 284–288.

Buchs, P.A., and Muller, D. (1996). Induction of long-term potentiation is associated with major ultrastructural changes of activated synapses. Proc. Natl. Acad. Sci. USA *93*, 8040–8045.

Capani, F., Martone, M.E., Deerinck, T.J., and Ellisman, M.H. (2001). Selective localization of high concentrations of F-actin in subpopulations of dendritic spines in rat central nervous system: a three-dimensional electron microscopic study. J. Comp. Neurol. *435*, 156–170.

Carlier, M.F., and Pantaloni, D. (1997). Control of actin dynamics in cell motility. J. Mol. Biol. *269*, 459–467.

Carroll, R.C., Beattie, E.C., von Zastrow, M., and Malenka, R.C. (2001). Role of AMPA receptor endocytosis in synaptic plasticity. Nat. Rev. Neurosci. *2*, 315–324.

Chen, H., Bernstein, B.W., and Bamburg, J.R. (2000). Regulating actin-filament dynamics in vivo. Trends Biochem. Sci. *25*, 19–23.

Colicos, M.A., Collins, B.E., Sailor, M.J., and Goda, Y. (2001). Remodeling of synaptic actin induced by photoconductive stimulation. Cell *107*, 605–616.

Cooper, J.A. (1987). Effects of cytochalasin and phalloidin on actin. J. Cell Biol. *105*, 1473–1478.

Cremona, O., and De Camilli, P. (2001). Phosphoinositides in membrane traffic at the synapse. J. Cell Sci. *114*, 1041–1052.

Edwards, D.C., Sanders, L.C., Bokoch, G.M., and Gill, G.N. (1999). Activation of LIM-kinase by Pak1 couples Rac/Cdc42 GTPase signalling to actin cytoskeletal dynamics. Nat. Cell Biol. *1*, 253–259.

Engert, F., and Bonhoeffer, T. (1999). Dendritic spine changes associated with hippocampal long-term synaptic plasticity. Nature *399*, 66–70.

Errington, M.L., Lynch, M.A., and Bliss, T.V. (1987). Long-term potentiation in the dentate gyrus: induction and increased glutamate release are blocked by D(-)aminophosphonovalerate. Neuroscience *20*, 279–284.

Fifkova, E. (1985). Actin in the nervous system. Brain Res. *356*, 187–215.

Fifkova, E., and Morales, M. (1992). Actin matrix of dendritic spines, synaptic plasticity, and long-term potentiation. Int. Rev. Cytol. *139*, 267–307.

Fischer, M., Kaech, S., Knutti, D., and Matus, A. (1998). Rapid actin-based plasticity in dendritic spines. Neuron *20*, 847–854.

Fischer, M., Kaech, S., Wagner, U., Brinkhaus, H., and Matus, A. (2000). Glutamate receptors regulate actin-based plasticity in dendritic spines. Nat. Neurosci. *3*, 887–894.

Frey, U., Huang, Y.Y., and Kandel, E.R. (1993). Effects of cAMP simulate a late stage of LTP in hippocampal CA1 neurons. Science *260*, 1661–1664.

Frey, U., Frey, S., Schollmeier, F., and Krug, M. (1996). Influence of actinomycin D, a RNA synthesis inhibitor, on long-term potentiation in rat hippocampal neurons in vivo and in vitro. J. Physiol. *490*, 703–711.

Geinisman, Y., Detoledo, M.L., Morrell, F., Persina, I.S., and Beatty, M.A. (1996). Synapse restructuring associated with the maintenance phase of hippocampal long-term potentiation. J. Comp. Neurol. *368*, 413–423.

Gomez, L.L., Alam, S., Smith, K.E., Horne, E., and Dell'Acqua, M.L. (2002). Regulation of A-kinase anchoring protein 79/150-cAMP-dependent protein kinase postsynaptic targeting by NMDA receptor activation of calcineurin and remodeling of dendritic actin. J. Neurosci. *22*, 7027–7044.

Halpain, S. (2000). Actin and the agile spine: how and why do dendritic spines dance? Trends Neurosci. *23*, 141–146.

Hayashi, Y., Shi, S.H., Esteban, J.A., Piccini, A., Poncer, J.C., and

Malinow, R. (2000). Driving AMPA receptors into synapses by LTP and CaMKII: requirement for GluR1 and PDZ domain interaction. Science *287*, 2262–2267.

Hjorth, S.A. (1972). Projection of the lateral part of the entorhinal area to the hippocampus and fascia dentata. J. Comp. Neurol. *146*, 219–232.

Hjorth, S.A., and Jeune, B. (1972). Origin and termination of the hippocampal perforant path in the rat studied by silver impregnation. J. Comp. Neurol. *144*, 215–232.

Inokuchi, K., Kato, A., Hirai, K., Hishinuma, F., Inoue, M., and Ozawa, F. (1996). Increase in activin beta A mRNA in rat hippocampus during long-term potentiation. FEBS Lett. *382*, 48–52.

Kaech, S., Parmar, H., Roelandse, M., Bornmann, C., and Matus, A. (2001). Cytoskeletal microdifferentiation: a mechanism for organizing morphological plasticity in dendrites. Proc. Natl. Acad. Sci. USA *98*, 7086–7092.

Kato, A., Ozawa, F., Saitoh, Y., Hirai, K., and Inokuchi, K. (1997). vesl, a gene encoding VASP/Ena family related protein, is upregulated during seizure, long-term potentiation and synaptogenesis. FEBS Lett. *412*, 183–189.

Kato, A., Ozawa, F., Saitoh, Y., Fukazawa, Y., Sugiyama, H., and Inokuchi, K. (1998). Novel members of the Vesl/Homer family of PDZ proteins that bind metabotropic glutamate receptors. J. Biol. Chem. *273*, 23969–23975.

Kim, C.H., and Lisman, J.E. (1999). A role of actin filament in synaptic transmission and long-term potentiation. J. Neurosci. *19*, 4314–4324.

Krucker, T., Siggins, G.R., and Halpain, S. (2000). Dynamic actin filaments are required for stable long-term potentiation (LTP) in area CA1 of the hippocampus. Proc. Natl. Acad. Sci. USA *97*, 6856–6861.

Krug, M., Lossner, B., and Ott, T. (1984). Anisomycin blocks the late phase of long-term potentiation in the dentate gyrus of freely moving rats. Brain Res. Bull. *13*, 39–42.

Langford, G.M., and Molyneaux, B.J. (1998). Myosin V in the brain: mutations lead to neurological defects. Brain Res. Brain Res. Rev. *28*, 1–8.

Link, W., Konietzko, U., Kauselmann, G., Krug, M., Schwanke, B., Frey, U., and Kuhl, D. (1995). Somatodendritic expression of an immediate early gene is regulated by synaptic activity. Proc. Natl. Acad. Sci. USA *92*, 5734–5738.

Lisman, J.E., and Zhabotinsky, A.M. (2001). A model of synaptic memory: a CaMKII/PP1 switch that potentiates transmission by organizing an AMPA receptor anchoring assembly. Neuron *31*, 191–201.

Lledo, P.-M., Zhang, X., Sudhof, T.C., Malenka, R.C., and Nicoll, R.A. (1998). Postsynaptic membrane fusion and long-term potentiation. Science *279*, 399–403.

Lyford, G.L., Yamagata, K., Kaufmann, W.E., Barnes, C.A., Sanders, L.K., Copeland, N.G., Gilbert, D.J., Jenkins, N.A., Lanahan, A.A., and Worley, P.F. (1995). Arc, a growth factor and activity-regulated gene, encodes a novel cytoskeleton-associated protein that is enriched in neuronal dendrites. Neuron *14*, 433–445.

Maekawa, M., Ishizaki, T., Boku, S., Watanabe, N., Fujita, A., Iwamatsu, A., Obinata, T., Ohashi, K., Mizuno, K., and Narumiya, S. (1999). Signaling from Rho to the actin cytoskeleton through protein kinases ROCK and LIM-kinase. Science *285*, 895–898.

Maletic-Savatic, M., Malinow, R., and Svoboda, K. (1999). Rapid dendritic morphogenesis in CA1 hippocampal dendrites induced by synaptic activity. Science *283*, 1923–1927.

Malinow, R., Mainen, Z.F., and Hayashi, Y. (2000). LTP mechanisms: from silence to four-lane traffic. Curr. Opin. Neurobiol. *10*, 352–357.

Matsuo, R., Kato, A., Sakaki, Y., and Inokuchi, K. (1998). Cataloging altered gene expression during rat hippocampal long-term potentiation by means of differential display. Neurosci. Lett. *244*, 173–176.

Matsuo, R., Murayama, A., Saitoh, Y., Sakaki, Y., and Inokuchi, K. (2000). Identification and cataloging of genes induced by long-lasting long-term potentiation in awake rats. J. Neurochem. *74*, 2239–2249.

Matsushita, M., Tomizawa, K., Moriwaki, A., Li, S.T., Terada, H., and Matsui, H. (2001). A high-efficiency protein transduction system demonstrating the role of PKA in long-lasting long-term potentiation. J. Neurosci. *21*, 6000–6007.

Matsuzaki, M., Ellis-Davies, G.C., Nemoto, T., Miyashita, Y., Iino, M., and Kasai, H. (2001). Dendritic spine geometry is critical for AMPA receptor expression in hippocampal CA1 pyramidal neurons. Nat. Neurosci. *4*, 1086–1092.

Matus, A. (2000). Actin-based plasticity in dendritic spines. Science *290*, 754–758.

Matus, A., Ackermann, M., Pehling, G., Byers, H.R., and Fujiwara, K. (1982). High actin concentrations in brain dendritic spines and postsynaptic densities. Proc. Natl. Acad. Sci. USA *79*, 7590–7594.

McNaughton, B.L. (1980). Evidence for two physiologically distinct perforant pathways to the fascia dentata. Brain Res. *199*, 1–19.

McNaughton, B.L., and Barnes, C.A. (1977). Physiological identification and analysis of dentate granule cell responses to stimulation of the medial and lateral perforant pathways in the rat. J. Comp. Neurol. *175*, 439–454.

Meberg, P.J., and Bamburg, J.R. (2000). Increase in neurite outgrowth mediated by overexpression of actin depolymerizing factor. J. Neurosci. *20*, 2459–2469.

Meng, Y., Zhang, Y., Tregoubov, V., Janus, C., Cruz, L., Jackson, M., Lu, W.Y., MacDonald, J.F., Wang, J.Y., Falls, D.L., and Jia, Z. (2002). Abnormal spine morphology and enhanced LTP in LIMK-1 knockout mice. Neuron *35*, 121–133.

Moriyama, K., Iida, K., and Yahara, I. (1996). Phosphorylation of Ser-3 of cofilin regulates its essential function on actin. Genes Cells *1*, 73–86.

Nakayama, A.Y., Harms, M.B., and Luo, L. (2000). Small GTPases Rac and Rho in the maintenance of dendritic spines and branches in hippocampal pyramidal neurons. J. Neurosci. *20*, 5329–5338.

Nedivi, E., Hevroni, D., Naot, D., Israeli, D., and Citri, Y. (1993). Numerous candidate plasticity-related genes revealed by differential cDNA cloning. Nature *363*, 718–721.

Nguyen, P.V., and Kandel, E.R. (1996). A macromolecular synthesis-dependent late phase of long-term potentiation requiring cAMP in the medial perforant pathway of rat hippocampal slices. J. Neurosci. *16*, 3189–3198.

Nguyen, P.V., Abel, T., and Kandel, E.R. (1994). Requirement of a critical period of transcription for induction of a late phase of LTP. Science *265*, 1104–1107.

Niwa, R., Nagata-Ohashi, K., Takeichi, M., Mizuno, K., and Uemura, T. (2002). Control of actin reorganization by Slingshot, a family of phosphatases that dephosphorylate ADF/cofilin. Cell *108*, 233–246.

Ostroff, L.E., Fiala, J.C., Allwardt, B., and Harris, K.M. (2002). Polyribosomes redistribute from dendritic shafts into spines with enlarged synapses during LTP in developing rat hippocampal slices. Neuron *35*, 535–545.

Pak, D.T., Yang, S., Rudolph-Correia, S., Kim, E., and Sheng, M. (2001). Regulation of dendritic spine morphology by SPAR, a PSD-95-associated RapGAP. Neuron *31*, 289–303.

Pantaloni, D., Le Clainche, C., and Carlier, M.F. (2001). Mechanism of actin-based motility. Science *292*, 1502–1526.

Patterson, R.L., van Rossum, D.B., and Gill, D.L. (1999). Store-operated Ca2+ entry: evidence for a secretion-like coupling model. Cell *98*, 487–499.

Penzes, P., Johnson, R.C., Sattler, R., Zhang, X., Huganir, R.L., Kambampati, V., Mains, R.E., and Eipper, B.A. (2001). The neuronal Rho-GEF Kalirin-7 interacts with PDZ domain-containing proteins and regulates dendritic morphogenesis. Neuron *29*, 229–242.

Qian, Z., Gilbert, M.E., Colicos, M.A., Kandel, E.R., and Kuhl, D. (1993). Tissue-plasminogen activator is induced as an immediate-early gene during seizure, kindling, and long-term potentiation. Nature *361*, 453–457.

Qualmann, B., Kessels, M.M., and Kelly, R.B. (2000). Molecular links between endocytosis and the actin cytoskeleton. J. Cell Biol. *150*, 111F–116F.

Schafer, D.A. (2002). Coupling actin dynamics and membrane dynamics during endocytosis. Curr. Opin. Cell Biol. *14*, 76–81.

Sheng, M., Lee, S.H., Kaech, S., Parmar, H., Roelandse, M., Bornmann, C., and Matus, A. (2001). AMPA receptor trafficking and the control of synaptic transmission. Cell *105*, 825–828.

Shi, S.H., Hayashi, Y., Petralia, R.S., Zaman, S.H., Wenthold, R.J., Svoboda, K., and Malinow, R. (1999). Rapid spine delivery and redistribution of AMPA receptors after synaptic NMDA receptor activation. Science *284*, 1811–1816.

Shi, S., Hayashi, Y., Esteban, J.A., and Malinow, R. (2001). Subunit-specific rules governing AMPA receptor trafficking to synapses in hippocampal pyramidal neurons. Cell *105*, 331–343.

Simone, N.L., Remaley, A.T., Charboneau, L., Petricoin, E.F., 3rd, Glickman, J.W., Emmert-Buck, M.R., Fleisher, T.A., and Liotta, L.A. (2000). Sensitive immunoassay of tissue cell proteins procured by laser capture microdissection. Am. J. Pathol. *156*, 445–452.

Spector, I., Shochet, N.R., Blasberger, D., and Kashman, Y. (1989). Latrunculins-novel marine macrolides that disrupt microfilament organization and affect cell growth: I. Comparison with cytochalasin D. Cell Motil. Cytoskeleton *13*, 127–144.

Star, E.N., Kwiatkowski, D.J., and Murthy, V.N. (2002). Rapid turnover of actin in dendritic spines and its regulation by activity. Nat. Neurosci. *5*, 239–246.

Steward, O. (1976). Topographic organization of the projections from the entorhinal area to the hippocampal formation of the rat. J. Comp. Neurol. *167*, 285–314.

Steward, O., Wallace, C.S., Lyford, G.L., and Worley, P.F. (1998). Synaptic activation causes the mRNA for the IEG Arc to localize selectively near activated postsynaptic sites on dendrites. Neuron *21*, 741–751.

Takiguchi, H.K., Sato, M., Sugo, N., Ishida, M., Sato, K., Uratani, Y., and Arimatsu, Y. (1998). Latexin expression in smaller diameter primary sensory neurons in the rat. Brain Res. *801*, 9–20.

Tashiro, A., Minden, A., and Yuste, R. (2000). Regulation of dendritic spine morphology by the rho family of small GTPases: antagonistic roles of Rac and Rho. Cereb. Cortex *10*, 927–938.

Toni, N., Buchs, P.A., Nikonenko, I., Bron, C.R., and Muller, D. (1999). LTP promotes formation of multiple spine synapses between a single axon terminal and a dendrite. Nature *402*, 421–425.

Toshima, J., Toshima, J.Y., Amano, T., Yang, N., Narumiya, S., and Mizuno, K. (2001). Cofilin phosphorylation by protein kinase testicular protein kinase 1 and its role in integrin-mediated actin reorganization and focal adhesion formation. Mol. Biol. Cell *12*, 1131–1145.

Trachtenberg, J.T., Chen, B.E., Knott, G.W., Feng, G., Sanes, J.R., Welker, E., and Svoboda, K. (2002). Long-term in vivo imaging of experience-dependent synaptic plasticity in adult cortex. Nature *420*, 788–794.

Trommald, M., Hulleberg, G., and Andersen, P. (1996). Long-term potentiation is associated with new excitatory spine synapses on rat dentate granule cells. Learn. Mem. *3*, 218–228.

van Rossum, D., and Hanisch, U.K. (1999). Cytoskeletal dynamics in dendritic spines: direct modulation by glutamate receptors? Trends Neurosci. *22*, 290–295.

Weeks, A., Ivanco, T.L., LeBoutillier, J.C., Racine, R.J., and Petit, T.L. (1998). The degree of potentiation is associated with synaptic number during the maintenance of long-term potentiation in the rat dentate gyrus. Brain Res. *798*, 211–216.

Wu, G.Y., Deisseroth, K., and Tsien, R.W. (2001). Spaced stimuli stabilize MAPK pathway activation and its effects on dendritic morphology. Nat. Neurosci. *4*, 151–158.

Yamagata, K., Andreasson, K.I., Kaufmann, W.E., Barnes, C.A., and Worley, P.F. (1993). Expression of a mitogen-inducible cyclooxygenase in brain: regulation by synaptic activity and glucocorticoids. Neuron *11*, 371–386.

Yamagata, K., Andreasson, K.I., Sugiura, H., Maru, E., Dominique, M., Irie, Y., Miki, N., Hayashi, Y., Yoshioka, M., Kaneko, K., et al. (1999). Arcadlin is a neural activity-regulated cadherin involved in long term potentiation. J. Biol. Chem. *274*, 19473–19479.

Yamazaki, M., Matsuo, R., Fukazawa, Y., Ozawa, F., and Inokuchi, K. (2001). Regulated expression of an actin-associated protein, synaptopodin, during long-term potentiation. J. Neurochem. *79*, 192–199.

Yang, N., Higuchi, O., Ohashi, K., Nagata, K., Wada, A., Kangawa, K., Nishida, E., and Mizuno, K. (1998). Cofilin phosphorylation by LIM-kinase 1 and its role in Rac-mediated actin reorganization. Nature *393*, 809–812.

Zhou, Q., Xiao, M.-Y., and Nicoll, R.A. (2001). Contribution of cytoskeleton to the internalization of AMPA receptors. Proc. Natl. Acad. Sci. USA *98*, 1261–1266.

Ziff, E.B. (1997). Enlightening the postsynaptic density. Neuron *19*, 1163–1174.